Molecular and functional characterisation of the zebrafish (*Danio rerio*) PEPT1-type peptide transporter[1]

Tiziano Verri[a,*], Gabor Kottra[b], Alessandro Romano[a], Natascia Tiso[c], Mark Peric[b], Michele Maffia[a], Michael Boll[b], Francesco Argenton[c], Hannelore Daniel[b], Carlo Storelli[a]

[a] *Laboratory of General Physiology, Department of Biological and Environmental Sciences and Technologies, University of Lecce, via Provinciale Lecce-Monteroni, I-73100 Lecce, Italy*
[b] *Institute of Nutritional Sciences, Technical University of Munich, Hochfeldweg 2, D-85350 Freising-Weihenstephan, Germany*
[c] *Department of Biology, University of Padua, via U. Bassi 58/B, I-35131 Padua, Italy*

Received 27 May 2003; revised 30 June 2003; accepted 30 June 2003

First published online 25 July 2003

Edited by Maurice Montal

Abstract **We report the molecular and functional characterisation of a novel peptide transporter from zebrafish, orthologue to mammalian and avian PEPT1. Zebrafish PEPT1 is a low-affinity/high-capacity system. However, in contrast to higher vertebrate counterparts in which maximal transport activity is independent of extracellular pH, zebrafish PEPT1 maximal transport rates unexpectedly increase at alkaline extracellular pH. Zebrafish *pept1* is highly expressed in the proximal intestine since day 4 post-fertilisation, thus preceding functional maturation of the gut, first feeding and complete yolk resorption. Zebrafish PEPT1 might help to understand the evolutionary and functional relationships among vertebrate peptide transporters. Moreover, zebrafish *pept1* can be a useful marker for screening mutations that affect gut regionalisation, differentiation and morphogenesis.**

Key words: Intestine; Peptide transport; Two-electrode voltage clamp; Whole-mount in situ hybridisation; Gut morphogenesis; *Xenopus laevis* oocytes

1. Introduction

Uptake of di- and tripeptides into cells is mediated by integral plasma membrane transport proteins with unique structural motifs, that belong to the peptide transporter family (PTR family)[1]. Members of this family have been characterised in bacteria, fungi, plants, fruitfly, *Caenorhabditis elegans*, birds and mammals. In higher vertebrates, two peptide transporters, namely PEPT1 [2–7] and PEPT2 [8–11], have been identified. These proteins are predominantly expressed in epithelial cells of small intestine, mammary gland, lung, choroid plexus and kidney, but are also present in other cell types (for a recent review, see [12]). They transport di- and tripeptides, with a preference for those containing L-amino acids, and a variety of peptidomimetics such as β-lactam antibiotics (penicillins and cephalosporins), aminopeptidase inhibitors (bestatin), angiotensin-converting enzyme inhibitors (captopril and enalapril), δ-aminolevulinic acid and selected prodrugs [12]. By coupling to the movement of protons down an inwardly directed electrochemical proton gradient, PEPT1 and PEPT2 allow substrate translocation across the plasma membrane against a concentration gradient. By virtue of this mechanism, substrate uptake responds to extracellular pH and membrane potential, and exhibits a pH optimum varying between 4.5 and 6.5, also depending on the net charge of the transported substrate (for detailed analyses in mammalian systems, see [13–18]).

In lower vertebrates, members of the PTR family have not yet been described at the molecular level. Due to their phylogenetic position, fish might represent a useful link to allow new insights into the molecular structure and function of vertebrate peptide transporters. We therefore aimed to identify peptide transport systems in zebrafish (*Danio rerio*), a teleost fish established as a powerful model organism for experimental biology, vertebrate embryology, developmental genetics and toxicology and of growing importance in regulatory and integrative physiology [19–21]. We here report the molecular and functional characterisation of the intestinal zebrafish PEPT1-type peptide transporter. Although structurally/functionally similar to the mammalian counterparts, zebrafish PEPT1 exhibits an unusual pH dependence with neutral to alkaline pH increasing its maximal transport rate. Expression of zebrafish *pept1* occurs early in the proximal intestinal epithelium during larval development, starting day 4 post-fertilisation.

2. Materials and methods

2.1. Fish breeding and embryo collection

Adult zebrafish were bred by natural crosses in a male to female ratio of 2:1 [22]. Immediately after spawning, the bottoms of the aquariums were siphoned. The fertilised eggs were harvested, washed and placed in 9 cm diameter Petri dishes in 0.6 mg/l Instant Ocean sea salts (Aquarium Systems, Sarrebourg, France). The developing embryos were incubated at 28.5°C until use. Developmental stages of zebrafish embryos were expressed as days post-fertilisation (dpf) at 28.5°C [23].

*Corresponding author. Fax: (39)-832-324220.
E-mail address: physiol@ultra5.unile.it (T. Verri).

[1] Sequence data submission and accession numbers: Sequence data reported are available in the DDBJ/EMBL/GenBank databases under accession nos. AY300011 (zebrafish *pept1*) and AY300010 (zebrafish *transketolase*).

Abbreviations: dpf, days post-fertilisation; PEPT1, peptide transporter 1; PEPT2, peptide transporter 2; PTR family, peptide transporter family; TEVC, two-electrode voltage clamp

0014-5793/03/$22.00 © 2003 Published by Elsevier B.V. on behalf of the Federation of European Biochemical Societies.
doi:10.1016/S0014-5793(03)00759-2

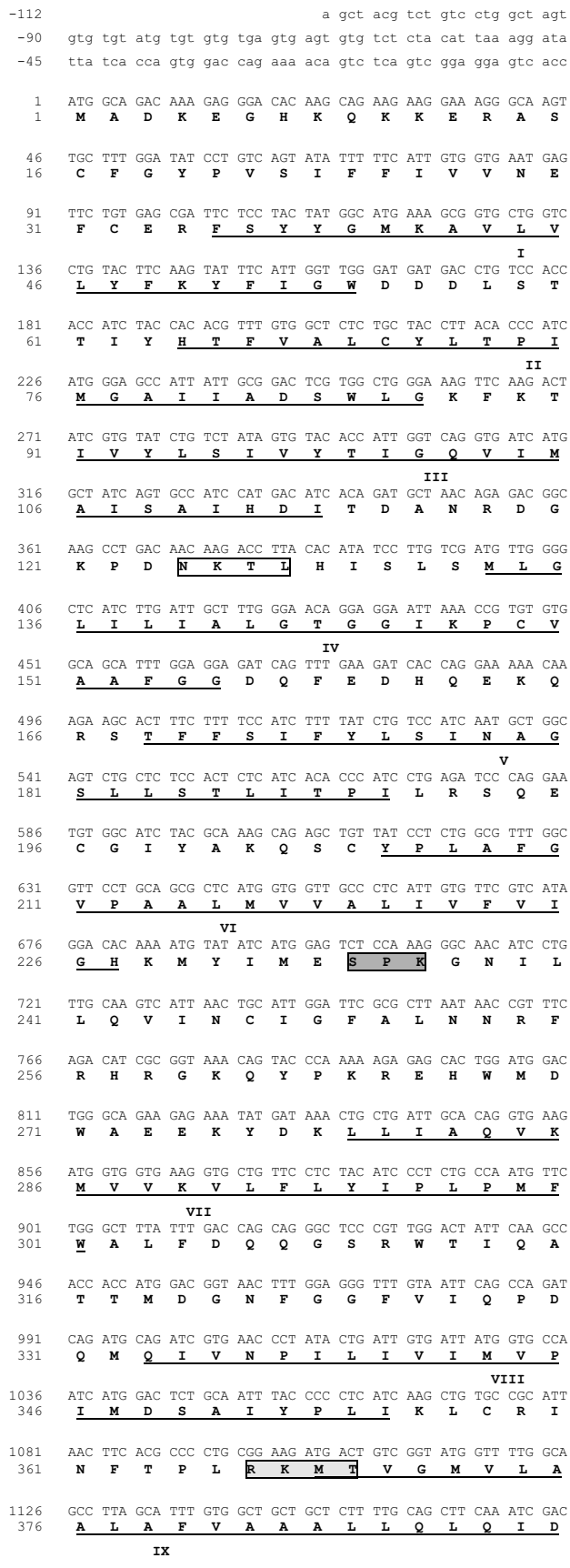
-112 a gct acg tct gtc ctg gct agt
-90 gtg tgt atg tgt gtg tga gtg agt gtg tct cta cat taa agg ata
-45 tta tca cca gtg gac cag aaa aca gtc tca gtc gga gga gtc acc
1 ATG GCA GAC AAA GAG GGA CAC AAG CAG AAG AAG GAA AGG GCA AGT
1 M A D K E G H K Q K K E R A S
46 TGC TTT GGA TAT CCT GTC AGT ATA TTT TTC ATT GTG GTG AAT GAG
16 C F G Y P V S I F F I V V N E
91 TTC TGT GAG CGA TTC TCC TAC TAT GGC ATG AAA GCG GTG CTG GTC
31 F C E R F S Y Y G M K A V L V
I
136 CTG TAC TTC AAG TAT TTC ATT GGT TGG GAT GAT GAC CTG TCC ACC
46 L Y F K Y F I G W D D D L S T
181 ACC ATC TAC CAC ACG TTT GTG GCT CTC TGC TAC CTT ACA CCC ATC
61 T I Y H T F V A L C Y L T P I
II
226 ATG GGA GCC ATT ATT GCG GAC TCG TGG CTG GGA AAG TTC AAG ACT
76 M G A I I A D S W L G K F K T
271 ATC GTG TAT CTG TCT ATA GTG TAC ACC ATT GGT CAG GTG ATC ATG
91 I V Y L S I V Y T I G Q V I M
III
316 GCT ATC AGT GCC ATC CAT GAC ATC ACA GAT GCT AAC AGA GAC GGC
106 A I S A I H D I T D A N R D G
361 AAG CCT GAC AAC AAG ACC TTA CAC ATA TCC TTG TCG ATG TTG GGG
121 K P D N K T L H I S L S M L G
406 CTC ATC TTG ATT GCT TTG GGA ACA GGA GGA ATT AAA CCG TGT GTG
136 L I L I A L G T G G I K P C V
IV
451 GCA GCA TTT GGA GGA GAT CAG TTT GAA GAT CAC CAG GAA AAA CAA
151 A A F G G D Q F E D H Q E K Q
496 AGA AGC ACT TTC TTT TCC ATC TTT TAT CTG TCC ATC AAT GCT GGC
166 R S T F F S I F Y L S I N A G
V
541 AGT CTG CTC TCC ACT CTC ATC ACA CCC ATC CTG AGA TCC CAG GAA
181 S L L S T L I T P I L R S Q E
586 TGT GGC ATC TAC GCA AAG CAG AGC TGT TAT CCT CTG GCG TTT GGC
196 C G I Y A K Q S C Y P L A F G
631 GTT CCT GCA GCG CTC ATG GTG GTT GCC CTC ATT GTG TTC GTC ATA
211 V P A A L M V V A L I V F V I
VI
676 GGA CAC AAA ATG TAT ATC ATG GAG TCT CCA AAG GGC AAC ATC CTG
226 G H K M Y I M E S P K G N I L
721 TTG CAA GTC ATT AAC TGC ATT GGA TTC GCG CTT AAT AAC CGT TTC
241 L Q V I N C I G F A L N N R F
766 AGA CAT CGC GGT AAA CAG TAC CCA AAA AGA GAG CAC TGG ATG GAC
256 R H R G K Q Y P K R E H W M D
811 TGG GCA GAA GAG AAA TAT GAT AAA CTG CTG ATT GCA CAG GTG AAG
271 W A E E K Y D K L L I A Q V K
856 ATG GTG GTG AAG GTG CTG TTC CTC TAC ATC CCT CTG CCA ATG TTC
286 M V V K V L F L Y I P L P M F
VII
901 TGG GCT TTA TTT GAC CAG CAG GGC TCC CGT TGG ACT ATT CAA GCC
301 W A L F D Q Q G S R W T I Q A
946 ACC ACC ATG GAC GGT AAC TTT GGA GGG TTT GTA ATT CAG CCA GAT
316 T T M D G N F G G F V I Q P D
991 CAG ATG CAG ATC GTG AAC CCT ATA CTG ATT GTG ATT ATG GTG CCA
331 Q M Q I V N P I L I V I M V P
VIII
1036 ATC ATG GAC TCT GCA ATT TAC CCC CTC ATC AAG CTG TGC CGC ATT
346 I M D S A I Y P L I K L C R I
1081 AAC TTC ACG CCC CTG CGG AAG ATG ACT GTC GGT ATG GTT TTG GCA
361 N F T P L R K M T V G M V L A
1126 GCC TTA GCA TTT GTG GCT GCT GCT CTT TTG CAG CTT CAA ATC GAC
376 A L A F V A A A L L Q L Q I D
IX
1171 GAA ACA ATG CCC AAG TTC CCA TCA ACC TCT CAA ACC CAG TTG AAG
391 E T M P K F P S T S Q T Q L K
1216 TTC CTG AAC GTT GAG AGC ACA TCA TTG CCT GTT GTA GTG GAG GGA
406 F L N V E S T S L P V V V E G
1261 CAA GAT CAA TTC ATG GTT CCT GGA TTC AAT GCC TCA AGT GAA TAC
421 Q D Q F M V P G F N A S S E Y
1306 TTG ACC CTG GAC AAG GAG AAT GTG ACC ATC TCT GCT GGA GGA GTC
436 L T L D K E N V T I S A G G V
1351 AAT GAT ACA GCC TTT TTA AAG ACC GGC ACC AGG CAC ACA GTT TTA
451 N D T A F L K T G T R H T V L
1396 ATG AAT GCT GCT GGA ATG AGA AAT ACG CTC GAT GAC CTT ACT GAG
466 M N A A G M R N T L D D L T E
1441 AAA CCA GAG CAA GGC CTG AAT GCC ATT AGG TTT GTG AAT GGC TGG
481 K P E Q G L N A I R F V N G W
1486 GAG AAT CGG CTG AAT GTG TCA GTG AAG TCT GAT AAT GTG CAC GCG
496 E N R L N V S V K S D N V H A
1531 GAT CCC CTG GAT GCA TCA GTT TAC TTA TTG GTT CCC CAT GGC AAA
511 D P L D A S V Y L L V P H G K
1576 GTC AAC TTT ACA ATT TTT GAC GGG GGC GAC GGG AAG TGC CAC TAC
526 V N F T I F D G G D G K C H Y
1621 ATT ATG CAG CTG GGC TTT GGA AGC ACT TAC ACA GTC CTG ATC CCC
541 I M Q L G F G S T Y T V L I P
(XIII)
1666 AGC ACC TTC GCC TTC GGA CAA ACT TGC AGC GAG AGC TTT GAA GCA
556 S T F A F G Q T C S E S F E A
1711 GTG CAG GAC ATG GAG CCC AAT AGG ATC CAC ATG GCC TGG CAG GTC
571 V Q D M E P N R I H M A W Q V
1756 ATT CAA TAC TTC CTT TTG ACC TGT GGT GAA GTG GTG TAC TCG GTC
586 I Q Y F L L T C G E V V Y S V
X
1801 ACC GGC CTC GAC TTC TCC TAT TCA CAG GCT CCG AGC AAC ATG AAG
601 T G L D F S Y S Q A P S N M K
1846 TCG GTC CTG CAG GCT GGT TGG CTG TTG ACC GTC GCT GTG GGG AAC
616 S V L Q A G W L L T V A V G N
XI
1891 ATC ATT GTG CTC ATC GTG GCT GAA GCA GGA TCT CTT CCG GAT CAG
631 I I V L I V A E A G S L P D Q
1936 TGG GCT GAA TAT CTG CTG TTC GCG TCT CTT CTG GTG GCT GTG AGC
646 W A E Y L L F A S L L V A V S
1981 ATC ATC TTC GCC ATC ATG GCC TAC TTC TAC ACC TAT ATC GAC CCG
661 I I F A I M A Y F Y T Y I D P
XII
2026 AAT GAG ATC GAG GCT AAG TTT AAA GAG TTG GAG CCC GAG GAC AAG
676 N E I E A K F K E L E P E D K
2071 AAA AGG AAA GAA ATG CAA ATG ACG GCC AAA GAC AAT ATG GCG TAC
691 K R K E M Q M T A K D N M A Y
2116 GTA CAC AAT GAG AAC ACA AAC ATC AAG CAA ACC AAG ATC TAG aca
706 V H N E N T N I K Q T K I ***
2161 ctt ttt ttt tct tcc ctc ctg atc aga ggt gtt cca cgt cgt gac
2206 tga tcc agc att ttc tta aac agt taa gtg tgg gat ttg ttg tag
2251 cag aaa aga ttc tca aat cag ccc aag gaa atg cta att ctt cct
2296 aaa ttg aag ttt tgt ttg gga tga aga gtg tgg gct tga ggg ttg
2341 gta gtt ttg gag ggt atc aga ctg tta atg tgt cac tat cgt gtg
2386 atg gtg act tta ttt atg agt cta tta tgt tac tat caa taa att
2431 gat gga tcg aaa caa gtg ttg ctc tga caa ttg act ctt atc atg
2476 gaa aaa cag tta aaa aat taa att taa agt gaa aaa aaa aaa aaa
2521 aaa a

2.2. Plasmids

The EST cDNA clone (GenBank accession no. AW175007) for zebrafish PEPT1 was purchased from the IMAGE Consortium (IMAGE clone no. 2639231). The insert was cut off its original plasmid pME18S-FL3 by *Eco*RI and *Xba*I and subcloned into pSPORT1 (Invitrogen, Carlsbad, CA, USA). The recombinant clone (zfPepT1-pSPORT1) was used for further analyses. Both strands of the cDNA insert were sequenced using 20-*mer* synthetic oligonucleotides (Proligo France, Paris, France). The resulting sequence was deposited in the GenBank database (GenBank accession no. AY300011).

2.3. Computer analysis

Zebrafish PEPT1 amino acid sequence was deduced using the open reading frame (ORF) finder program at http://www.ncbi.nlm.nih.gov. Putative transmembrane domains and potential *N*-glycosylation, cAMP-dependent protein kinase and protein kinase C recognition sequences were defined using the PROSITE 17.0 computational tools. Sequence similarity search was performed by FASTA 3.39. Multiple sequence alignments were obtained by Clustal W 1.82. The phylogenetic reconstruction was generated by the neighbour-joining method [24], as implemented in MEGA 2.1 [25]. GenBank accession nos. for sequence comparisons are: U06467 (rabbit PEPT1; [2]), U13173 (human PEPT1; [3]), D50664 (rat PEPT1; [4]), AF205832 (mouse PEPT1; [5]), AY027496 (sheep PEPT1; [6]), AY029615 (chicken PEPT1; [7]), U32507 (rabbit PEPT2; [10]), S78203 (human PEPT2; [8]), D63149 (rat PEPT2; [9]) and NM_021301 (mouse PEPT2; [11]).

2.4. Expression in Xenopus laevis oocytes and electrophysiology

Female clawed frogs (*X. laevis*) were purchased from Nasco (Fort Atkinson, WI, USA). To collect oocytes, the animals were anaesthetised by immersion in 0.7 g/l MS-222 (3-aminobenzoic acid ethyl ester; Sigma, St. Louis, MO, USA). Surgical procedures were performed as described [26]. After the final collection, the frogs were killed with an anaesthetic overdose. Oocytes were treated with 2.5 mg/ml collagenase for 90 min, separated manually and incubated in Barth's solution containing (in mM): 88 NaCl, 1 KCl, 0.8 $MgSO_4$, 0.4 $CaCl_2$, 0.3 $Ca(NO_3)_2$, 2.4 $NaHCO_3$ and 10 HEPES (pH 7.5) at 17°C overnight. Stage V/VI oocytes were injected with 9 ng (in 14 nl) of in vitro synthesised zebrafish *pept1*-specific cRNA (Ambion mMessage mMachine T7 kit; AMS, Wiesbaden, Germany) and incubated for 3–6 days at 17°C.

Two-electrode voltage clamp (TEVC) experiments were performed as described [17]. Briefly, the oocyte was placed in an open chamber (~0.5 ml total volume) and continuously superfused (~3 ml/min) with the Barth's solution or with solutions containing the substrate dipeptide. Electrodes with resistance between 1 and 10 MΩ were connected to a TEC-05 amplifier (npi electronic, Tamm, Germany). Oocytes were voltage clamped at −60 mV, and current–voltage (*I–V*) relations were measured using short (100 ms) pulses separated by 200 ms pauses in the potential range −160 to +80 mV. *I–V* measurements were made immediately before and 30–40 s after substrate application when current flow reached steady state. The zebrafish PEPT1-evoked current at a given membrane potential was calculated as the difference between the currents measured in the presence and absence of substrate. *I–V* relations were calculated with a Visual Basic routine written in Microsoft Excel. Positive currents denote positive charges flowing out of the oocyte.

Gly-L-Gln (Sigma) was added to the solutions in concentrations as indicated in the text. After addition of the dipeptide, the pH was adjusted if necessary. The percentage of the zwitterionic form at a given pH was calculated with p*K* values taken from [27] (for Gly-L-Gln, $pK_1 = 2.88$ and $pK_2 = 8.29$).

Transport parameters, i.e. apparent Gly-L-Gln affinity ($K_{0.5}$; mM) and maximal transport current (I_{max}; nA), were calculated on the basis of the Michaelis–Menten equation from at least three and preferably four to five data points. pH dependence of I_{max} was determined in paired experiments, i.e. each oocyte was perfused with solutions having pH values of 8.5, 7.5, 6.5 and 5.5. At each pH value, in addition to the substrate-free control solution, two substrate concentrations were applied, one high concentration (up to 20 mM) evoking near-maximal current and one concentration near to the respective pH-dependent $K_{0.5}$ value which was determined in preceding experiments. The sequence of pH values was varied to avoid systematic errors. Data are the mean ± S.E.M. of *n* experiments. Statistically significant differences ($P < 0.05$) were determined using the Student's *t*-test for paired or non-paired data as appropriate.

2.5. Reverse transcription-polymerase chain reaction (RT-PCR)

Total RNA was extracted from either tissues of adult animals or 1–7 dpf embryos (TRIzol Reagent; Invitrogen). Adult fish were anaesthetised by immersion in 0.2 g/l MS-222 and then killed by decapitation prior to organ removal. Embryos were killed by anaesthetic overdose. RT-PCR was performed using the GeneAmp Gold RNA PCR Reagent kit (Applied Biosystems, Foster City, CA, USA). RT was performed (42°C/12 min) in the presence of oligo$(dT)_{16}$ and PCR using zebrafish *pept1*-specific primers (forward: 5′-GACTCGTGGCTGGGAAAGTTC-3′, starting at nucleotide 244; reverse: 5′-AGTATAGGGTTCACGATCTG-3′, starting at nucleotide 1016; Fig. 1). Amplification was performed for 35 cycles (95°C denaturation/30 s, 55°C annealing/1 min, 72°C extension/1 min; final synthesis: 72°C/7 min). Analogously, for *β-actin*-specific RNA, RT was performed (42°C/12 min) in the presence of oligo$(dT)_{16}$ and PCR using zebrafish *β*-actin-specific primers (GenBank accession no. NM_131031; forward: 5′-CGTGACATCAAGGAGAAGCT-3′, starting at nucleotide 681; reverse: 5′-ATCCACATCTGCTGGAAGGT-3′, starting at nucleotide 1123). Amplification was performed for 35 cycles (95°C denaturation/30 s, 50°C annealing/1 min and 72°C extension/1 min; final synthesis: 72°C/7 min). RT-PCR products were separated on a 1% agarose gel and stained by ethidium bromide.

2.6. Whole-mount in situ hybridisation

A 205 bp fragment corresponding to a portion of zebrafish PEPT1 large extracellular loop between the transmembrane domains IX and X was amplified by PCR from zfPepT1-pSPORT1 using the following *pept1*-specific primers (forward: 5′-TGTGACCATCTCTGCTGGAG-3′, starting at nucleotide 1326; reverse: 5′-CCGCGTGCACATTATCAGAC-3′, starting at nucleotide 1531; Fig. 1). The amplification product was subcloned into the pCRII-TOPO (TOPO TA Cloning, Invitrogen) and the recombinant clone (zfOL-pCRII-TOPO) sequenced to confirm the identity of the insert. The 205 bp digoxigenin (DIG)-11-UTP (Roche, Mannheim, Germany)-labelled antisense riboprobe was synthesised in vitro with T7 RNA polymerase (Roche) using the *Hin*dIII-cleaved zfOL-pCRII-TOPO. Whole-mount in situ hybridisation was performed as described [28]. Stained embryos were dehydrated with methanol, clarified in benzyl benzoate:benzyl alcohol (2:1, v/v) and mounted in glycerol. Embryos were observed on a Leica DMR microscope equipped with Nomarski optics and a DC500 Leica digital camera.

3. Results

3.1. Sequence analysis

Zebrafish *pept1* cDNA was 2746 bp long, with an ORF of 2157 bp encoding a putative protein of 718 amino acids (Fig. 1). Hydropathy analysis predicts at least 12 potential membrane spanning domains with a large extracellular loop between transmembrane domains IX and X (Fig. 1). Six putative extracellular *N*-glycosylation sites, two intracellular consensus regions containing protein kinase C motifs and one intracellular cAMP-dependent protein kinase sequence were identified (Fig. 1). When compared to members of the

←

Fig. 1. Nucleotide and predicted amino acid sequence. Numbers on the left refer to the nucleotide (upper row) and amino acid (lower row) positions. Nucleotides are numbered, starting from the first ATG initiation codon within a strong Kozak consensus sequence. *** indicates the stop codon. A polyadenylation signal is double underlined. In the amino acid sequence, putative transmembrane domains are underlined (–) and named I to XII. In addition, a potentially hydrophobic region is also underlined (- - -) and named (XIII). Potential extracellular *N*-glycosylation sites (white boxes) and potential cAMP-dependent protein kinase (grey box) and protein kinase C (dark boxes) phosphorylation sites at the cytoplasmic surface are indicated.

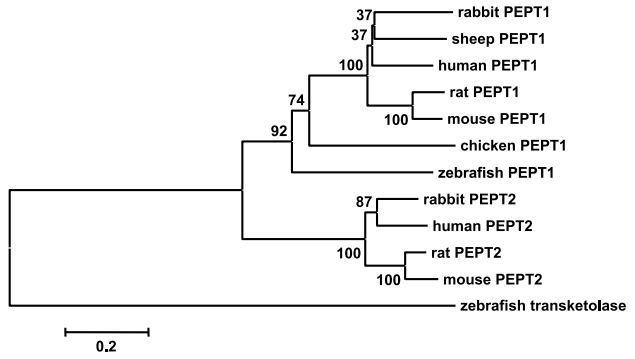

Fig. 2. Phylogenetic tree built on the alignment of the complete amino acid sequences of known vertebrate peptide transporters. The bootstrap values (1000 replicates) are reported above each branch in the figure. The sequence of zebrafish transketolase (GenBank accession no. AY300010) was used as an outgroup in the phylogenetic reconstruction.

PTR family already characterised from other vertebrates, the predicted zebrafish PEPT1 amino acid sequence exhibits a higher percentage of identity with the PEPT1-type (60.3–61.5%) than with the PEPT2-type (45.5–48.9%) transporters. The phylogenetic reconstruction of vertebrate peptide transporter proteins clustered zebrafish PEPT1 to the PEPT1 branch of the phylogenetic tree and indicated early divergence of the fish protein sequence with respect to those of the tetrapod group (Fig. 2).

3.2. Function

The zwitterionic dipeptide Gly-L-Gln, a well-known high-affinity substrate for mammalian PEPT1 transporters, was used as a test compound in TEVC experiments to establish the basic kinetic properties of the zebrafish transporter (Fig. 3). *I–V* relations were measured 30–40 s after the start of the superfusion of oocytes (clamped at −60 mV) with 1 and 20 mM Gly-L-Gln at the extracellular pH value of 7.5 (Fig. 3A) and did not differ substantially from those obtained with rabbit PEPT1 under identical experimental conditions [17]. At pH 7.5 the transport current was inwardly directed at negative membrane potentials. However, the direction of current reversed (i.e. it became outwardly directed) at more positive membrane potentials (at −7 and +47 mV when 1 and 20 mM Gly-L-Gln were applied, respectively). This finding suggests that zebrafish PEPT1, similarly to the mammalian orthologues, transports electrogenically not only in the forward but also in the reverse direction. $K_{0.5}$ and I_{max} determined using extracellular Gly-L-Gln concentrations ranging between 0.5 and 5 mM at pH 7.5 and at two different membrane potentials are shown (Fig. 3B and Table 1). Comparison of these with previously published results shows that the rabbit and zebrafish transporters exhibit comparable $K_{0.5}$ for Gly-L-

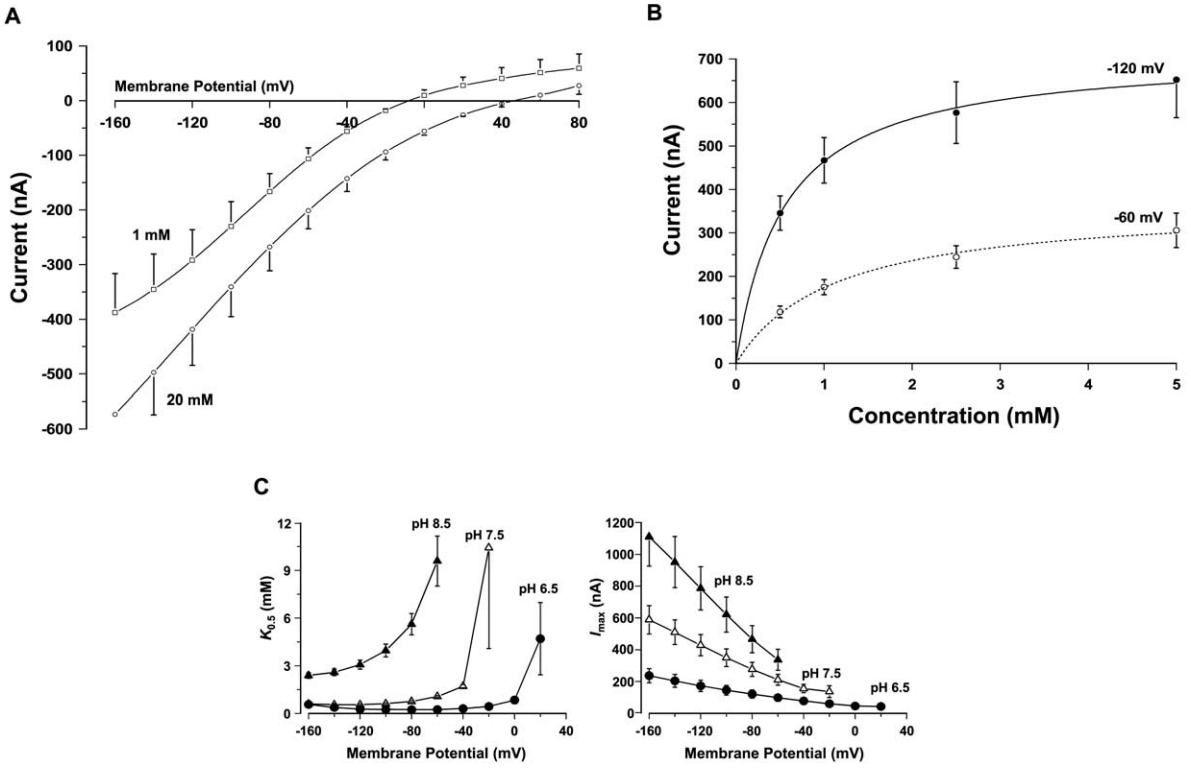

Fig. 3. Electrophysiological characterisation of zebrafish PEPT1-expressing *X. laevis* oocytes. A: Steady-state current–voltage (*I–V*) relationships for Gly-L-Gln (1 and 20 mM, pH 7.5; $n = 10$). Note that the reversal potential for 1 mM is negative, i.e. the substrate concentration inside must have been higher than outside. B: Peptide-evoked inward currents as a function of Gly-L-Gln concentration (0.5–5 mM, pH 7.5) at two different membrane potentials (−60 and −120 mV; $n = 10$). C: Kinetic parameters (apparent Gly-L-Gln affinity, $K_{0.5}$, and maximal transport current, I_{max}) of inwardly directed Gly-L-Gln transport as a function of membrane potential and pH. Zebrafish PEPT1-expressing oocytes were perfused at pH 6.5 ($n = 10$), 7.5 ($n = 10$) or 8.5 ($n = 10$) in the presence of increasing Gly-L-Gln concentrations (0.5–20 mM). At each substrate concentration, steady-state *I–V* relationships were recorded and currents obtained replotted as a function of Gly-L-Gln concentration. Data were fitted to a Michaelis–Menten equation by non-linear regression analysis using the least-squares method and $K_{0.5}$ and I_{max} values of Gly-L-Gln calculated for each individual membrane potential. Note that the minimum of $K_{0.5}$ is shifted towards more positive membrane potentials with decreasing pH.

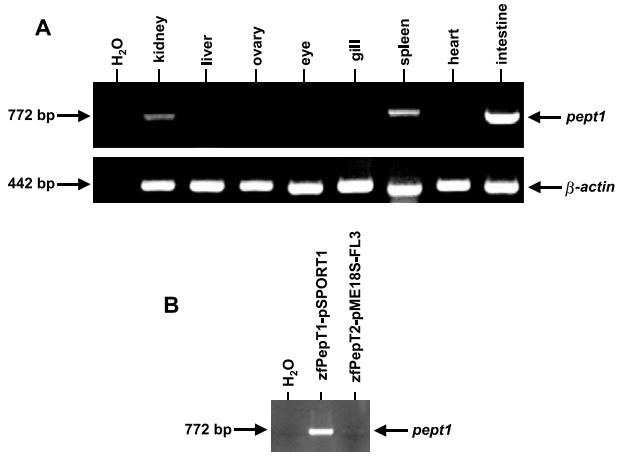

Fig. 4. Tissue distribution of zebrafish *pept1* in adult fish. A: RT-PCR performed on equal amounts of total RNA (1 μg) isolated from adult fish tissues using either zebrafish *pept1*- or zebrafish *β-actin*-specific primers (see Section 2). H_2O indicates no RNA in RT (negative control). B: PCR on control plasmids to assess primer specificity; no plasmid, H_2O; zebrafish *pept1* cDNA, zfPepT1-pSPORT1 (5 ng; positive control); zebrafish *pept2* cDNA, zfPepT2-pME18S-FL3 (5 ng; negative control). zfPepT2-pME18S-FL3 is an EST clone (GenBank accession no. AW153469) from the IMAGE Consortium (IMAGE clone no. 2601882) containing a partial zebrafish *pept2* cDNA.

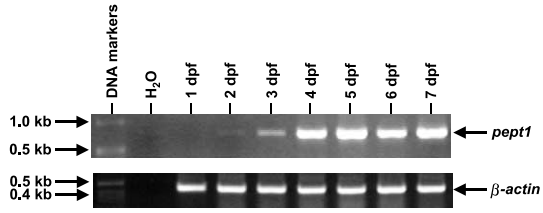

Fig. 5. Expression of zebrafish *pept1* in zebrafish embryos. RT-PCR performed on equal amounts of total RNA (2 μg) isolated from 1–7 dpf embryos using either zebrafish *pept1*- or zebrafish *β-actin*-specific primers (see Section 2). H_2O indicates no RNA in RT (negative control). DNA markers indicates 1 kb DNA ladder (Invitrogen, Carlsbad, CA, USA).

Gln in the millimolar range. In fact, $K_{0.5}$ at −60 mV and pH 7.5 was 1.06 mM for zebrafish PEPT1 and 0.70 mM for rabbit PEPT1 [17] and both values decreased to 0.55 mM for zebrafish PEPT1 and to 0.42 mM for rabbit PEPT1 [18], at −120 mV. The dependencies of $K_{0.5}$ and I_{max} on membrane potential and extracellular pH are presented in Fig. 3C. $K_{0.5}$ values were strongly affected by both membrane potential and pH. At each membrane potential, apparent affinity for Gly-L-Gln at pH 6.5 was always higher than that at pH 7.5 and both were significantly higher (at least 10-fold) than that measured at pH 8.5 (Fig. 3C, left panel). However, the 'real' affinity differences might be lower, when only the neutral form of Gly-L-Gln (98% at pH 6.5, 86% at pH 7.5, but only 38% at pH 8.5; Table 1) was transported. In this case, the measured $K_{0.5}$ values would be overestimated by 2%, 16% and 163% at pH 6.5, 7.5 and 8.5, respectively. At each external pH, $K_{0.5}$ displayed a membrane potential-dependent minimum, which was shifted towards depolarising membrane potentials with decreasing pH, i.e. <-160 mV at pH 8.5, −120 mV at pH 7.5 and −80 mV at pH 6.5. A further depolarisation below these potentials induced a sharp reduction in apparent substrate affinity (Fig. 3C, left panel). This behaviour was very similar to that observed with the rabbit transporter [17]. On the other side, as expected from an electrogenic transporter, I_{max} also exhibited a clear dependence on membrane potential and its value steadily decreased passing from −160 mV to less negative potentials at each external pH (Fig. 3C, right panel). Varying extracellular pH from 6.5 to 8.5 resulted, unexpectedly, in a pronounced increase (at least four-fold) of the maximal transport current (Fig. 3C, right panel). This increase in I_{max} as the external proton concentration decreases is, to our knowledge, the first description of such a kinetic behaviour in any of the PEPT-type transporters. Thus, in spite of several similarities, a striking difference exists between the kinetic behaviour of zebrafish PEPT1 and that of the other known mammalian peptide transporters. Kinetic parameters as a function of extracellular pH at −60 and −120 mV are reported in Table 1.

3.3. *Tissue distribution of zebrafish* pept1 *in adult fish*

Using zebrafish *pept1*-specific primers, a 772 bp RT-PCR product was amplified from total RNA isolated from the intestine of adult zebrafish, as well as from the kidney and spleen (Fig. 4). Under our experimental conditions, no signal was obtained in samples of ovary, eye, heart, liver and gill. As a control to assess RNA quality, *β-actin* RNA amplification was performed using zebrafish *β-actin*-specific primers, which invariably gave comparable 442 bp amplification products for all tested tissues (Fig. 4).

3.4. *Expression of zebrafish* pept1 *during larval development*

Zebrafish *pept1* expression (Fig. 5) was analysed during larval development by RT-PCR, using the same primers and

Table 1
pH dependence of the kinetic parameters of inwardly directed Gly-L-Gln transport via zebrafish PEPT1 by TEVC experiments

pH	Neutral form (%)	Oocytes clamped at −60 mV			Oocytes clamped at −120 mV		
		$K_{0.5}$ (mM)	I_{max} (%)	Number of experiments, *n*/*N*	$K_{0.5}$ (mM)	I_{max} (%)	Number of experiments, *n*/*N*
5.5	99.6	0.16 ± 0.05	41.0 ± 4.3	9/2	n.m.	n.m.	–
6.5	98.4	0.24 ± 0.07	43.4 ± 3.4	10/2	0.27 ± 0.06	37.7 ± 3.1	10/2
7.5	86.0	1.06 ± 0.06	100	10/2	0.55 ± 0.06	100	10/2
8.5	38.1	9.58 ± 1.57	161.8 ± 10.0	10/2	3.07 ± 1.57	183.0 ± 7.0	10/2

Kinetic parameters (apparent Gly-L-Gln affinity, $K_{0.5}$, and maximal transport current, I_{max}) were calculated at −60 and at −120 mV by least-squares fit to the Michaelis–Menten equation (see Fig. 3C). I_{max} values are expressed as the percentage of I_{max} calculated at pH 7.5 in the same experiment. The percentage of the dipeptide present in its neutral (zwitterionic) form was calculated as described in Section 2. Due to the decreasing concentration of zwitterionic species at increasing pH values $K_{0.5}$ could be overestimated at pH 8.5 (see Section 3). *n* and *N* specifies the number of oocytes and frogs, respectively. At pH 5.5 data could not be evaluated in oocytes clamped at −120 mV due to a large conductance of unknown origin (unfavourable conditions for the oocyte, i.e. low pH and hyperpolarisation); n.m. = non measurable.

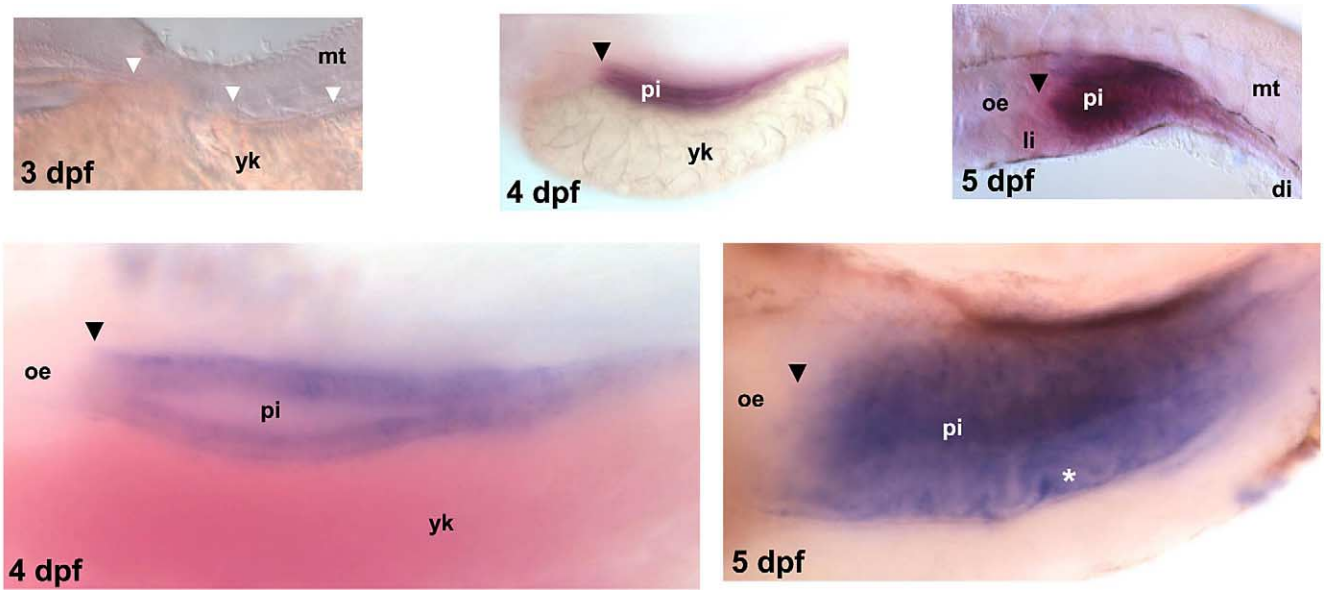

Fig. 6. In situ expression pattern of zebrafish *pept1* in 3–5 dpf zebrafish embryos. In each picture, anterior is to the left. All views are lateral with dorsal to the top. pi, proximal intestine; di, distal intestine; oe, oesophagus; li, liver; yk, yolk; mt, miotome; black arrowheads in the 4 and 5 dpf embryo pictures indicate the oesophageal–intestinal junction; white arrowheads in 3 dpf embryo picture indicates the location of the developing (immature) gut. The white asterisk indicates proximal intestinal folding.

similar experimental conditions as described above with *β-actin* RNA amplification serving as control. A very faint signal for zebrafish *pept1*-specific mRNA could be detected already at day 2 post-fertilisation. This signal slightly increased at day 3 and reached maximal values at days 4–7 post-fertilisation. Zebrafish *pept1* expression was also analysed by whole-mount in situ hybridisation, using a specific antisense riboprobe (see Section 2). Specific labelling was detected in 4 and 5 dpf embryos, but not in 3 dpf embryos (Fig. 6) or embryos at earlier stages of development (1–2 dpf; data not shown). In particular, in situ analysis confirmed that zebrafish *pept1* is abundantly expressed in the intestinal tube starting at day 4 post-fertilisation. From day 4 onwards, high levels of transcript were detected in the columnar epithelium of the proximal intestine, while no mRNA could be detected in the distal intestine or other tissues/organs of the developing embryo (Fig. 6). A similar pattern of expression also resulted using another (375 bp) riboprobe specific for a segment of the 3′ untranslated region of zebrafish *pept1* (data not shown).

4. Discussion

By screening EST databases, we have identified a cDNA encoding for a novel functional zebrafish peptide transporter of the PTR family [1]. The protein, designated as zebrafish PEPT1, represents the orthologue of mammalian and avian PEPT1 proteins. In fact, when compared to other known members of the PTR family in vertebrates, the predicted amino acid sequence of zebrafish PEPT1 (a) shares a significantly higher overall identity to PEPT1- than to PEPT2-type transporters and (b) clusters to the PEPT1 monophyletic group of the reconstructed phylogenetic tree, giving rise to the more basal branch.

In the last decade, extensive functional analysis of the cloned mammalian PEPT1-type peptide transporters has been performed using the TEVC technique, which has allowed a detailed characterisation of the electrophysiological properties when expressed in *X. laevis* oocytes (see [13–15,17,18] and the literature cited therein). In the present study, this experimental approach has been used to determine the basic properties of zebrafish PEPT1 and the kinetic constants of substrate binding and translocation. In general terms, zebrafish PEPT1 represents a classical low-affinity/high-capacity system, which operates in an electrogenic mode with similar affinities for the model dipeptide Gly-L-Gln as the mammalian proteins.

As a novel finding, we observed a significant increase of I_{max} when extracellular pH was elevated from 6.5 to 8.5. This has never been registered in any of the vertebrate PEPT1 proteins, which under substrate saturation conditions operate essentially in a pH-independent manner. The pH dependence of the I_{max} of zebrafish PEPT1 represents a unique feature of the zebrafish transporter. Why zebrafish PEPT1 responds to extracellular alkalinisation with an increase in maximal transport activity is not known, but a possible explanation could be that the protein contains an extra inhibitory allosteric proton binding site that reduces the maximal transport activity at low pH. By this novel functional difference with respect to the mammalian counterparts, the zebrafish transporter could be an ideal model for molecular mapping of functionally important regions in the proteins by construction of chimeras from fish and mammalian transporters.

Zebrafish is a carnivorous fish, which has its functional correlate in the presence of a very short intestinal tract. Moreover, zebrafish is stomachless (i.e. no acidic content is released into the proximal intestine) and its intestinal lumen might be alkaline under normal physiological conditions (due to pancreas and gallbladder secretions into the intestinal lumen). That this holds true is supported by the finding of alkaline pH (higher than 7.5) in adult zebrafish intestinal lumen [29]. Also, we have measured alkaline intestinal pH (higher than 7.5) in vivo by allowing young (4–10 dpf) zebrafish larvae to swallow a 0.04% solution of the pH-indicator *m*-cresol purple

(data not shown). In mammals, the acidic microclimate layer occurring in the vicinity of the luminal cell surface of the small intestinal epithelium is important for optimal absorption of peptides via PEPT1 [12]. This process depends on the trans-apical pH gradient that is maintained, at least in part, by the activity of the brush-border membrane Na^+/H^+ exchanger NHE3 (for recent data, see [30,31]). It has recently been shown that NHE3 is not expressed in the intestine of the Osorezan dace *Tribolodon hakonensis* [32], a cyprinid taxonomically related to zebrafish. Therefore, no acidification process (at least via NHE3) might occur in cyprinids and, as a consequence, no acidic microclimate pH might be effective, thus making the external cell surface of the intestinal epithelium fully sense the luminal alkaline pH. In this respect, the presence of a low-affinity/high-capacity peptide transport system that is adapted to optimally operate at alkaline pH in the proximal part of the intestine would allow rapid and complete transport of peptides derived from intestinal protein digestion. Interestingly, the only other intestinal transporter cloned so far from zebrafish, the type-II Na^+-phosphate cotransporter [29], also exhibits maximal transport activation at alkaline extracellular pH, thus suggesting that zebrafish intestinal transporters might effectively be adapted to more alkaline pH under normal physiological conditions.

Zebrafish *pept1* is highly expressed in the intestine. Expression in the proximal intestine is found early during embryo development, starting by day 2 post-fertilisation and reaching high levels by day 4 post-fertilisation. Energy requirement of early zebrafish embryo is provided by the yolk, until full maturation of the gut occurs. The morphogenesis of zebrafish digestive tract occurs by 58 h post-fertilisation (hpf) (~2.5 dpf), long after the gut tube has formed and after the common ductular system of the liver and pancreas are contiguous with the digestive tract. At this stage, contiguous, histologically recognisable primordia of pharinx, oesophagus and intestine are present. Subsequently, there is further growth and differentiation of all digestive organ primordia such that, by day 5 post-fertilisation, the digestive system is functional and longitudinally differentiated in mouth and oral cavity, pharynx, oesophagus, intestine, rectum and anus [33]. Full patency of the rostral digestive tract is achieved by 74 hpf (~3 dpf), when the lumen of the posterior pharinx is visible and the mouth is open. The anus is open at 96 hpf (4 dpf). Epithelial polarisation occurs parallel to organ morphogenesis with markers of apical membranes of the intestinal cells (i.e. *β-actin* and alkaline phosphatase) first detected at 34 hpf and increasing from day 3 (the end of the hatching period) to day 4 post-fertilisation. By days 4 to 5, the anterior intestine also undergoes a transition from a straight to a coiled tube and exhibits typical folding. Our results indicate that zebrafish PEPT1 is already expressed in the proximal intestine at day 4 post-fertilisation with strong signals in proximal intestine and rostral expansion at day 5 and thereafter. It therefore appears that zebrafish PEPT1 expression precedes the functional maturation of the gut, which occurs at day 5 post-fertilisation and makes the fish ready to perform first feeding and digestion of external food. Also, at day 5 post-fertilisation the larva starts the active search for external food, although a remnant of the yolk is still present. Our results on zebrafish PEPT1 are in agreement with the spatio-temporal expression of intestinal fatty acid binding protein (*i-fabp*) gene, which is involved in intestinal fat absorption and metabolism. *i-fabp* is expressed in the intestinal tube around day 3 post-fertilisation. However, by day 4, high level of *i-fabp*-specific transcripts are found in the proximal columnar epithelium and from day 5 onwards *i-fabp* is strongly expressed in the proximal intestine [34]. Taken together, these data support the conclusion that the site of the most efficient nutrient absorption in zebrafish is the proximal intestine with the genes encoding the nutrient transporters expressed at high levels before the animals start to rely on external food.

In summary, a zebrafish intestinal PEPT1-type peptide transporter has been identified and characterised with respect to its spatio-temporal expression in the gut and its transport function. Zebrafish PEPT1 will contribute to study peptide transporters in a laboratory model and well-established genetic background. By its unique pH dependence, zebrafish PEPT1 might also be instrumental for a detailed analysis of domains within the proteins that confer certain functional characteristics.

Acknowledgements: This investigation was supported by the Italian Ministry for the Agriculture and Forestry Policies (Fifth Plan on Fisheries and Aquaculture) and National Research Council (CNR Target Project on Biotechnology).

References

[1] Steiner, H.Y., Naider, F. and Becker, J.M. (1995) Mol. Microbiol. 16, 825–834.
[2] Fei, Y.J., Kanai, Y., Nussberger, S., Ganapathy, V., Leibach, F.H., Romero, M.F., Singh, S.K., Boron, W.F. and Hediger, M.A. (1994) Nature 368, 563–566.
[3] Liang, R., Fei, Y.J., Prasad, P.D., Ramamoorthy, S., Han, H., Yang-Feng, T.L., Hediger, M.A., Ganapathy, V. and Leibach, F.H. (1995) J. Biol. Chem. 270, 6456–6463.
[4] Miyamoto, K., Shiraga, T., Morita, K., Yamamoto, H., Haga, H., Taketani, Y., Tamai, I., Sai, Y., Tsuji, A. and Takeda, E. (1996) Biochim. Biophys. Acta 1305, 34–38.
[5] Fei, Y.J., Sugawara, M., Liu, J.C., Li, H.W., Ganapathy, V., Ganapathy, M.E. and Leibach, F.H. (2000) Biochim. Biophys. Acta 1492, 145–154.
[6] Pan, Y., Wong, E.A., Bloomquist, J.R. and Webb Jr., K.E. (2001) J. Nutr. 131, 1264–1270.
[7] Chen, H., Pan, Y., Wong, E.A., Bloomquist, J.R. and Webb Jr., K.E. (2002) J. Nutr. 132, 387–393.
[8] Liu, W., Liang, R., Ramamoorthy, S., Fei, Y.J., Ganapathy, M.E., Hediger, M.A., Ganapathy, V. and Leibach, F.H. (1995) Biochim. Biophys. Acta 1235, 461–466.
[9] Saito, H., Okuda, M., Terada, T., Sasaki, S. and Inui, K.I. (1995) J. Pharm. Exp. Ther. 275, 1631–1637.
[10] Boll, M., Herget, M., Wagener, M., Weber, W.M., Markovich, D., Biber, J., Clauss, W., Murer, H. and Daniel, H. (1996) Proc. Natl. Acad. Sci. USA 93, 284–289.
[11] Rubio-Aliaga, I., Boll, M. and Daniel, H. (2000) Biochem. Biophys. Res. Commun. 276, 734–741.
[12] Rubio-Aliaga, I. and Daniel, H. (2002) Trends Pharmacol. Sci. 23, 434–440.
[13] Amasheh, S., Wenzel, U., Boll, M., Dorn, D., Weber, W.M., Clauss, W. and Daniel, H. (1997) J. Membrane Biol. 155, 247–256.
[14] Amasheh, S., Wenzel, U., Weber, W.M., Clauss, W. and Daniel, H. (1997) J. Physiol. 504, 169–174.
[15] Steel, A., Nussberger, S., Romero, M.F., Boron, W.F., Boyd, C.A.R. and Hediger, M.A. (1997) J. Physiol. 498, 563–569.
[16] Chen, X.Z., Zhu, T., Smith, D.E. and Hediger, M.A. (1999) J. Biol. Chem. 274, 2773–2779.
[17] Kottra, G. and Daniel, H. (2001) J. Physiol. 536, 495–503.
[18] Kottra, G., Stamfort, A. and Daniel, H. (2002) J. Biol. Chem. 277, 32683–32691.
[19] Dooley, K. and Zon, L.I. (2000) Curr. Opin. Gen. Dev. 10, 252–256.

[20] Farber, S.A., Pack, M., Ho, S.Y., Johnson, I.D., Wagner, D.S., Dosch, R., Mullins, M.C., Hendrickson, H.S., Hendrickson, E.K. and Halpern, M.E. (2001) Science 292, 1385–1388.
[21] Briggs, J.P. (2002) Am. J. Physiol. Regul. Integr. Comp. Physiol. 282, R3–R9.
[22] Westerfield, M. (1995) The Zebrafish Book. A Guide for the Laboratory Use of Zebrafish (*Danio rerio*), University of Oregon Press, Eugene, OR.
[23] Kimmel, C.B., Ballard, W.W., Kimmel, S.R., Ullmann, B. and Schilling, T.F. (1995) Dev. Dyn. 203, 253–310.
[24] Saitou, N. and Nei, M. (1987) Mol. Biol. Evol. 4, 406–425.
[25] Kumar, S., Tamura, K., Jakobsen, I.B. and Nei, M. (2001) Bioinformatics 17, 1244–1245.
[26] Romero, M.F., Kanai, Y., Gunshin, H. and Hediger, M.A. (1998) in: Methods in Enzymology (Amara, S.G., Ed.), Vol. 296, pp. 17–51, Academic Press, New York.
[27] Sober, M.A. (1968) CRC Handbook of Biochemistry, CRC Press, Cleveland, OH.
[28] Thisse, C., Thisse, B., Schilling, T.F. and Postlethwait, J.H. (1993) Development 119, 1203–1215.
[29] Nalbant, P., Boehmer, C., Dehmelt, L., Wehner, F. and Werner, A. (1999) J. Physiol. 520, 79–89.
[30] Thwaites, D.T., Kennedy, D.J., Raldua, D., Anderson, C.M., Mendoza, M.E., Bladen, C.L. and Simmons, N.L. (2002) Gastroenterology 122, 1322–1333.
[31] Kennedy, D.J., Leibach, F.H., Ganapathy, V. and Thwaites, D.T. (2002) Pflügers Arch. 445, 139–146.
[32] Hirata, T., Kaneko, T., Ono, T., Nakazato, T., Furukawa, N., Hasegawa, S., Wakabayashi, S., Shigekawa, M., Chang, M.H., Romero, M.F. and Hirose, S. (2003) Am. J. Physiol. Regul. Integr. Comp. Physiol. 284, R1199–R1212.
[33] Wallace, K.N. and Pack, M. (2003) Dev. Biol. 255, 12–29.
[34] André, M., Ando, S., Ballagny, C., Durliat, M., Poupard, G., Briançon, C. and Babin, P.J. (2000) Int. J. Dev. Biol. 44, 249–252.